西南交通大学学报

第 58 卷 第 5 期
2023 年 10 月

JOURNAL OF SOUTHWEST JIAOTONG UNIVERSITY

Vol. 58 No. 5
Oct. 2023

ISSN: 0258-2724 DOI：10.35741/issn.0258-2724.58.5.57

Research article

Materials Science

NANOINDENTATION STUDY OF SUPERHARD TISIN, DIAMOND-LIKE CARBON (DLC), AND TISIN/DLC HYBRID COATINGS ON TUNGSTEN CARBIDE CUTTING TOOLS

碳化钨切削刀具上超硬泰信、类金刚石碳(DLC)和钛辛/DLC混合涂层的纳米压痕研究

Nuntapol Vattanaprateep [a], Nurot Panich [b], Prayoon Surin [a,*]

[a] Department of Advanced Manufacturing Technology, Faculty of Engineering, Pathumwan Institute of Technology
Bangkok, Thailand, nuntapolvat@gmail.com, Prayoon@pit.ac.th

[b] Faculty of Engineering, Rajapark Institute
Bangkok, Thailand, nurotw@yahoo.com

Received: August 17, 2023 ▪ Review: August 23, 2023
▪ Accepted: September 17, 2023 ▪ Published: October 30, 2023

Abstract

The nanoindentation technique has emerged as a powerful method for precisely assessing the mechanical properties of materials such as hardness and modulus at the nanoscale. This paper elaborates the capabilities of nanoindentation to determine the intrinsic mechanical properties, particularly hardness and elastic modulus of advanced coatings TiSiN, DLC, and a novel TiSiN/DLC hybrid coating on tungsten carbide cutting tools. X-ray diffraction (XRD) analysis revealed unique peak orientations for each coating, with TiSiN and TiSiN/DLC hybrid coatings exhibiting a coating texture with preferred (111) and (200) orientations in achieving superior hardness. Raman analysis confirmed the DLC nature of the coatings. Calotest measurements demonstrated differences in coating thickness, with DLC being thinner than TiSiN and TiSiN/DLC coatings. Nanoindentation tests revealed that the TiSiN coatings displayed exceptional superhardness, with a hardness of 40.2 GPa and an elastic modulus of 405.2 GPa, whereas the TiSiN/DLC hybrid coatings showed notable improvements in hardness and elastic modulus compared with the DLC coatings, with a hardness of 32.2 GPa and an elastic modulus of 356.8 GPa. These findings underscore the mechanical strength of TiSiN coatings, making them suitable for the machining industry. The TiSiN/DLC hybrid coatings exhibit potential for various industrial applications. This research enhances our understanding of superhard coatings, contributing to surface engineering and the development of high-performance coatings.

Keywords: Nanoindentation, Superhard Coatings, Titanium Silicon Nitride Coatings, Diamond-Like Carbon Coatings, Titanium Silicon Nitride/Diamond-Like Carbon Hybrid Coatings

摘要 纳米压痕技术已成为精确评估纳米尺度材料的机械性能（例如硬度和模量）的强大方法。本文阐述了纳米压痕技术在确定碳化钨刀具上先进涂层氮化钛、DLC和新型氮化钛/DLC混合涂层的固有机械性能，特别是硬度和弹性模量方面的能力。X射线衍射(X射线衍射)分析揭示了每种涂层独特的峰取向，氮化钛和氮化钛/DLC混合涂层表现出具有优选(111)和(200)取向的涂层结构，可实现优异的硬度。拉曼分析证实了涂层的DLC性质。卡洛测试测量显示涂层厚度存在差异，DLC比氮化钛和氮化钛/DLC涂层更薄。纳米压痕测试表明，氮化钛涂层表现出优异的超硬度，硬度为40.2 GPa，弹性模量为405.2 GPa，而氮化钛/DLC杂化涂层与DLC涂层相比，硬度和弹性模量显着提高，硬度为 32.2 GPa，弹性模量356.8 GPa。这些发现强调了氮化钛涂层的机械强度，使其适用于机械加工行业。氮化钛/DLC混合涂层展现出各种工业应用的潜力。这项研究增强了我们对超硬涂层的理解，有助于表面工程和高性能涂层的开发。

关键词: 纳米压痕、超硬涂层、氮化钛硅涂层、类金刚石碳涂层、氮化钛硅/类金刚石碳混合涂层

I. INTRODUCTION

Rapid advancements in materials science and technology have fueled a growing demand for precise methods to assess the mechanical properties of materials, particularly in the industrial sector. Nanoindentation has emerged as a versatile and accurate technique for meeting these demands. This powerful method enables the measurement of mechanical properties at the nanoscale, providing valuable insights into a material's response to mechanical stress. Nanoindentation has found widespread applications across various industrial sectors and significantly advanced research in fields such as materials science, coatings technology, and biomaterials [1], [2].

Nanoindentation operates on a straightforward principle: a controlled load is applied to a sharp indenter, and the resulting penetration depth or displacement is continuously monitored. The relationship between the applied force and indentation depth is then analyzed to determine the critical mechanical properties. Typically, nanoindentation instruments feature a sharp indenter, commonly a diamond tip, a highly precise load actuator, and a displacement transducer, often in the form of a capacitive sensor. The load-displacement data from the test are analyzed using methods such as the Oliver-Pharr method to determine parameters such as hardness and elastic modulus [3], [4].

These instruments are equipped with advanced control and data acquisition systems, allowing the measurement of crucial mechanical properties, including hardness, elastic modulus, yield strength, creep resistance, and fracture toughness. These parameters play a vital role in evaluating a material's suitability for specific industrial applications, making nanoindentation an essential tool for quality control, materials development, and product enhancement. Nanoindentation has a profound impact on various industrial sectors by facilitating materials and coatings evaluation. Its versatility and precision make it indispensable for assessing mechanical properties in diverse applications. Whether it is optimizing the performance of cutting tools, evaluating the durability of surface coatings, or enhancing the quality of biomedical implants, nanoindentation significantly contributes to the advancement of industrial materials and processes. While nanoindentation is a powerful technique, it does have limitations, with measurement accuracy affected by factors such as substrate effects, indenter tip shape, and contact mechanics [5].

Recently, surface coatings have become a vital avenue for improving the properties of various materials. These coatings are specifically designed to enhance attributes such as hardness, modulus, wear resistance, friction, anti-corrosion capabilities, and high-temperature resistance. The use of Ti-based coatings, such as titanium nitride (TiN) coatings, has been instrumental in enhancing industrial tool performance. This success has led to the development of an entire family of TiN-based coatings [5], [6], including titanium aluminum nitride (TiAlN) [7], titanium silicon nitride (TiSiN) [6], [7], and multilayer coatings [8], [9].

Diamond-like carbon (DLC) coatings have also gained prominence across industries, demonstrating exceptional tribological properties. DLC coatings offer low friction, high wear resistance, and corrosion protection, making them invaluable in various applications [10]-[12].

This work primarily emphasizes the innovative TiSiN/DLC hybrid coating, which combines the strengths of TiSiN providing superior mechanical properties and exceptional hardness and DLC coatings providing enhanced surface smoothness and excellent tribological performance. This study explores the application of nanoindentation techniques to characterize the mechanical properties of TiSiN, DLC, and novel TiSiN/DLC hybrid coatings applied to tungsten carbide cutting tools, which are commonly used in various industrial sectors.

II. MATERIALS AND METHODS

The materials used in this study comprised tungsten carbide (WC) specimens, specifically of RSK15X grade, and cutting inserts as substrates. The tungsten carbide specimens were of dimensions 12 x 12 x 3 mm. For the experimental setup, thin films of titanium silicon nitride (TiSiN), diamond-like carbon (DLC), and the novel TiSiN/DLC hybrid coating were deposited onto the cutting inserts, as illustrated in Figure 1.

(a)

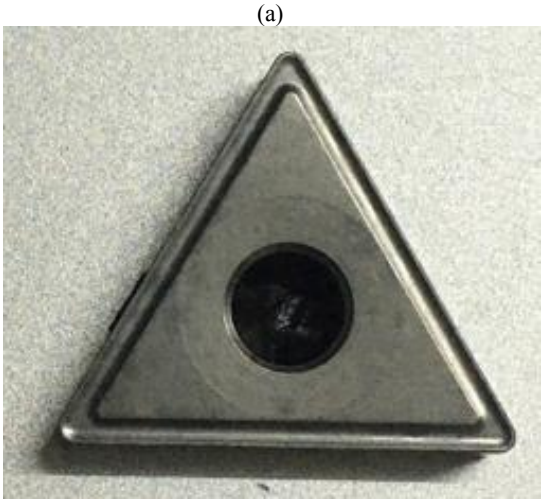

(b)

(c)

Figure 1. Cutting inserts deposited on (a) TiSiN, (b) DLC, and (c) TiSiN/DLC coatings (The authors)

An analysis of the elemental composition of the tungsten carbide (WC) substrate was conducted using energy-dispersive X-ray spectroscopy (EDS). This analytical technique provided insights into the substrate's elemental composition. The results of the EDS analysis are presented in Table 1, which details the weight percentages of various elements in the tungsten carbide (WC) substrate.

Table 1.
Elemental composition of the tungsten carbide (WC) substrate (The authors)

Substrate (WC)	W	C	Co	Si	Cr
% wt	78.81	7.75	11.15	1.67	0.62

In this study, tungsten carbide (WC) tool steel substrates were selected as the primary material for experimentation. To ensure a pristine surface, the specimens underwent manual grinding and polishing. Prior to their introduction into the deposition chamber, the WC substrates were subjected to ultrasonic cleaning with a combination of acetone and ethanol. The deposition process relied on a cathodic arc system provided by Diacoat Technologies Co., Ltd.

The deposition setup featured a cylindrical chamber housing three 4-inch water-cooled target holders, each tilted at an angle of approximately 30 degrees relative to the horizontal substrate holder's normal axis. The substrate holder can be heated using graphite heating elements. Throughout the experiments, a consistent working pressure of 0.65 Pa was maintained, with a total argon (Ar) gas flow rate of 20 standard cubic centimeters per minute (sccm). The substrate temperature was adjustable, ranging from room temperature (RT) to as high as 480 ºC. An RF power bias was employed for

effective sputter cleaning of the substrate surface.

Figure 2 shows a schematic illustrating the cathodic arc evaporation (CAE) process used for depositing the TiSiN coatings. This diagram serves as a visual guide to the deposition method. The process is detailed as follows. The TiSiN coating deposition started with a 5-min step for a pure titanium (Ti) layer. During this stage, the substrate was maintained at a bias voltage of -200 V, and the Ti cathode current varied between 120 and 140 A. Subsequently, the primary TiSiN top layer was deposited over an extended period of 90 min. This layer was created using a dedicated TiSi cathode, with arc currents ranging between 120 and 140 A. The bias voltages were adjusted between 8 and 130 A. Of significance is the continuous rotation of the substrate during all deposition phases, maintaining a consistent speed of 20 revolutions per minute (rpm). This rotation ensures a uniform and even distribution of the coating. Throughout the deposition process, the substrate temperature remained constant at 480ºC, ensuring appropriate conditions for the successful deposition of the TiSiN coatings.

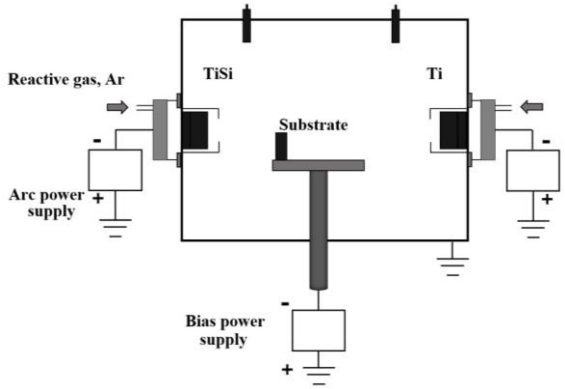

Figure 2. Schematic diagram of cathodic arc evaporation (The authors)

Figure 3 presents a schematic diagram that outlines the deposition process for both diamond-like carbon (DLC) and TiSiN/DLC hybrid coatings. This diagram provides a visual representation of the respective processes. The process details are as follows. The filtered cathodic vacuum arc (FCVA) method was employed. The process involved the sputtering of a Ti interlayer onto the substrate using DC magnetron sputtering. The substrate temperature was meticulously maintained at 170°C throughout the procedure. The distance between the substrate and Ti target was maintained at 80 mm. To establish an appropriate vacuum environment, the chamber was evacuated until it reached a base pressure of 3.0 x 10^{-3} Pa. The substrates were then subjected to a 20-min Ar ion etching process to ensure proper substrate preparation. During the deposition of the DLC coatings, the cathodes operated at a DC arc current that ranged from 60 to 100 A. A normal bias voltage of -1500 to -1700 V was applied during the deposition.

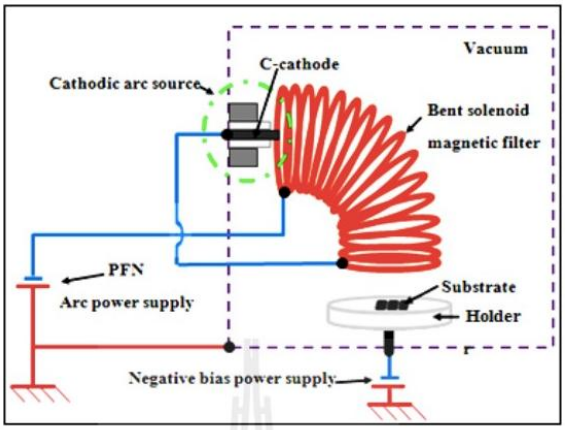

Figure 3. Schematic of the DLC and TiSiN/DLC coating deposition process (The authors)

To characterize the coatings, various techniques were employed. The phase identification of the resulting coatings was performed using a Rigaku X-ray diffractometer (Miniflex 2). Scanning electron microscopy (SEM) was conducted with a Quanta 450 instrument, and energy-dispersive spectroscopy (EDS) analysis was performed using the Oxford INCA-350 system. Coating thickness measurements were performed by creating a ball crater on the coating surface using the Calotest machine manufactured by Anton Paar. Surface roughness was examined using atomic force microscopy (AFM), and an indentation test was conducted using a Fischer HM2000 microhardness tester. A flowchart illustrating the characterization process for the coatings is presented in Figure 4.

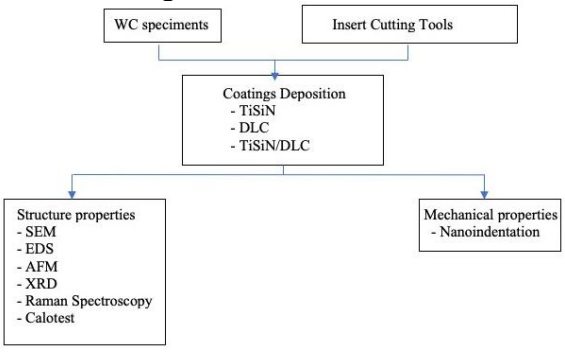

Figure 4. Flowchart of coating characterization (The authors)

III. Results and Discussion

A. SEM Analysis

To analyze the morphology of the TiSiN, DLC, and TiSiN/DLC hybrid coatings, we present the following figures:

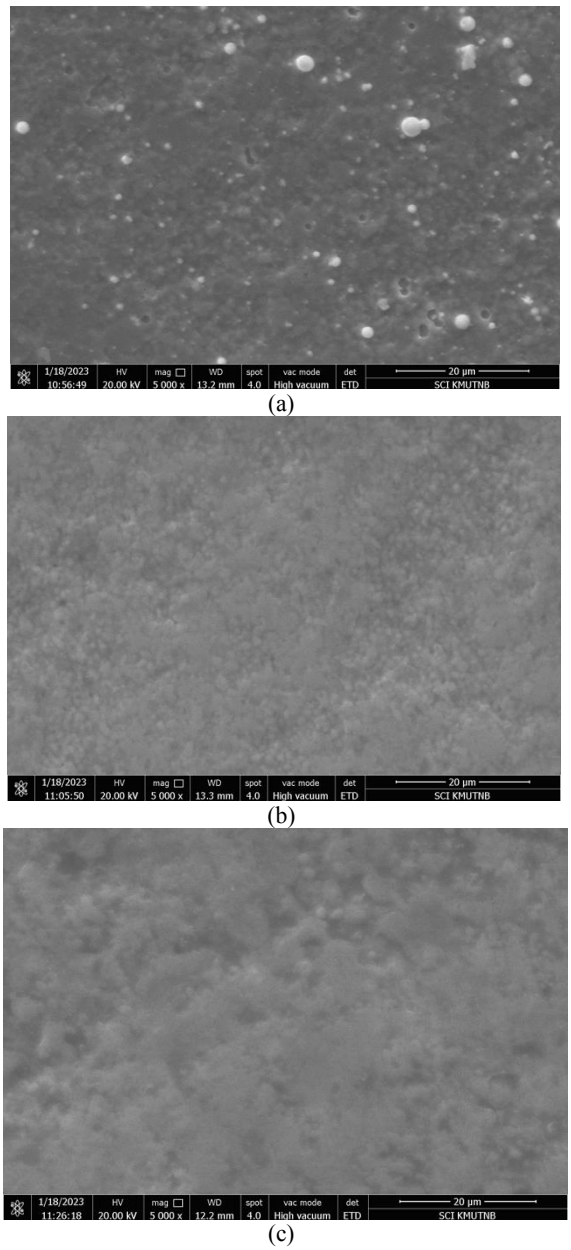

Figure 5. SEM of the morphology of (a) TiSiN, (b) DLC, and (c) TiSiN/DLC coatings (The authors)

Figure 5 provides scanning electron microscope (SEM) images illustrating the morphology of the resultant coatings. It is evident from these images that the surface morphologies of the TiSiN coatings exhibit several macroparticles. In contrast, the surface morphologies of the DLC and TiSiN/DLC coatings appear much smoother and show less porosity than that of the TiSiN coatings.

B. AFM Analysis

In Figure 6, we present atomic force microscope (AFM) images that further depict the morphology of the resultant coatings. These AFM images confirm the structure of the respective coatings. Notably, although TiSiN coatings exhibit higher surface roughness values, the AFM image reveals a dense morphology, contributing to their super high hardness compared with that of DLC coatings.

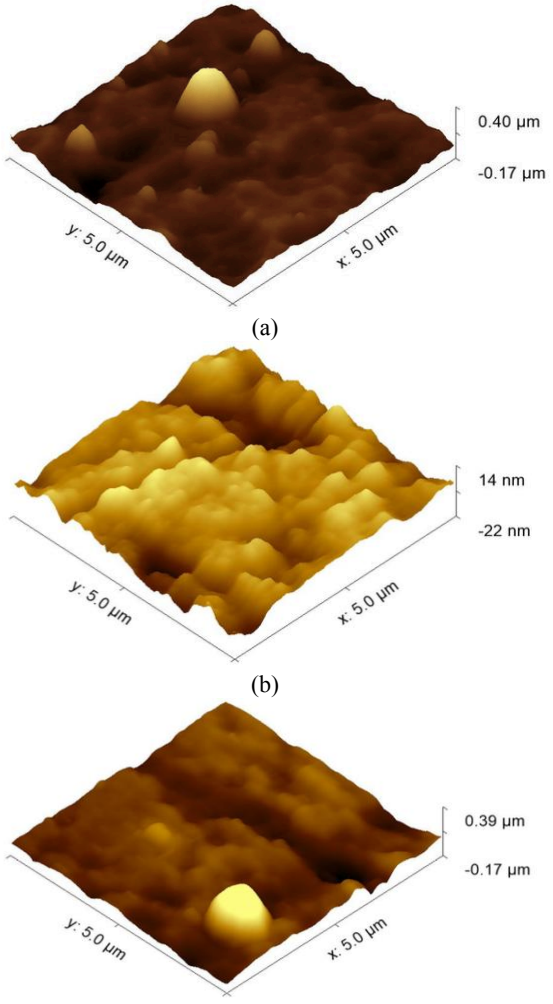

Figure 6. AFM of the morphology of (a) TiSiN, (b) DLC, and (c) TiSiN/DLC coatings (The authors)

The observed differences in surface morphology, as demonstrated by SEM and AFM images, play a significant role in the mechanical properties of these coatings. The dense morphology of TiSiN contributes to its exceptional hardness, making it suitable for various industrial applications. The smoother and less porous surfaces of the DLC and TiSiN/DLC hybrid coatings may indicate improved hardness and modulus, making them valuable in cutting tools or applications. In summary, the analysis of coating morphology provides valuable insights into the structure and properties of TiSiN, DLC, and TiSiN/DLC hybrid coatings. These findings are crucial for understanding their performance in various industrial applications.

C. XRD Analysis

XRD analysis was conducted to determine the crystallographic orientations and phases of the TiSiN, DLC, and TiSiN/DLC coatings. The data revealed the presence of specific crystallographic

orientations for each coating.

Figure 7 displays the XRD patterns of the TiSiN, DLC, and TiSiN/DLC coatings. The patterns show distinctive peaks associated with the crystallographic orientations of the coatings. Notably, the observed peak orientations for each coating are summarized in Table 2. Commonly observed peaks in the XRD pattern of TiSiN coatings include those associated with titanium nitride (TiN) and silicon nitride (Si_3N_4) phases. These peaks are typically indexed according to the Miller indices of the corresponding crystallographic planes. These observations contribute to our understanding of the structural properties and composition of the coatings, providing insights into their mechanical characteristics and potential applications. The presence of a single peak in the XRD patterns suggests a fiber texture with preferred (111), (110), and (200) orientations in the TiSiN coatings. This observation aligns with the findings in the literature, where most TiSiN coatings are reported to display hexagonal phase patterns with a preferred (111) and (200) orientation [6], [7]. (111) and (200) oriented coatings are known to yield the highest hardness. This trend is also observed in the DLC coatings. The (111) plane, which has the highest packing factor, requires energetic adatoms to create such an orientation.

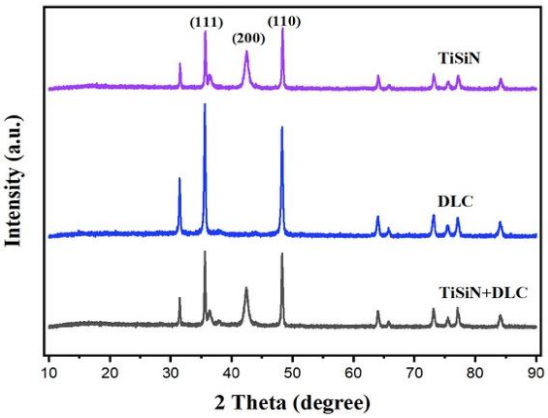

Figure 7. Patterns of XRD of the resultant coatings (The authors)

Table 2.
Thickness, surface roughness, and orientation of the resultant coatings (The authors)

Coatings	Thickness	Surface roughness		Orientation
		Mean	RMS	
	(μm)	(nm)	(nm)	
TiSiN	1.6	35.96	55.45	(111), (110), and (200)
DLC	1.0	5.65	7.75	(111) and (110)
TiSiN/DLC	1.8	24.60	36.74	(111), (110), and (200)

These findings underscore the significance of crystallographic orientation in influencing the mechanical properties of the coatings. Further research into optimizing orientation can have implications for the performance of TiSiN and DLC coatings.

D. Raman Analysis

Raman spectra were recorded to confirm the DLC nature of the deposited granular protrusions.

Figure 8 presents the Raman spectra of the specimen surfaces, showcasing the granular protrusions of carbon (C) and those with a C film without mask material. The Raman waveforms displayed two distinct peaks near 1540 cm^{-1} (G band) and 1330 cm^{-1} (D band). These characteristic peaks confirm the DLC nature of the deposited granular protrusions [10], [11]. This Raman analysis provides further evidence of the DLC nature of the coatings and is consistent with the expectations for DLC materials. The presence of G and D bands indicates the graphitic and disordered carbon structures commonly associated with DLC.

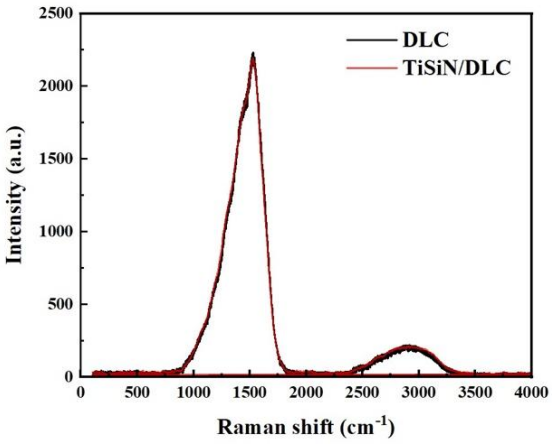

Figure 8. Patterns of Raman spectroscopy of the DLC and TiSiN/DLC coatings (The authors)

E. Calotest

Calotest analysis is a valuable technique for measuring the thickness of surface coatings. It offers precise and reliable measurements that are essential for quality control and ensuring coating uniformity in various industrial applications. This method is particularly well suited for industries where coating thickness plays a critical role in performance and durability, such as automotive,

aerospace, and surface engineering. The ability to accurately measure coating thickness is essential for meeting industry standards, optimizing performance, and ensuring the longevity of coated components in diverse industrial settings.

Figure 9 displays Calotest images of the coatings. The Calotest results revealed differences in the coating thickness. Specifically, the DLC coatings exhibited a thickness approximately 1 μm less than the other coatings. The TiSiN coatings had a thickness of approximately 1.6 μm, while the TiSiN/DLC hybrid coatings had a thickness of approximately 1.8 μm. These variations in coating thickness can have implications for the mechanical properties of the coatings and their suitability for specific applications.

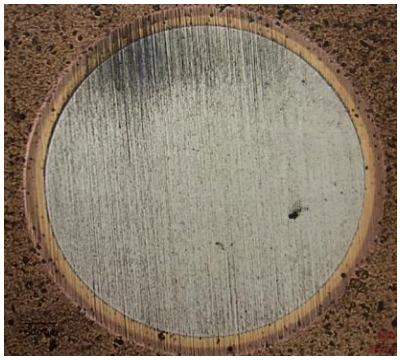

(a) TiSiN coatings

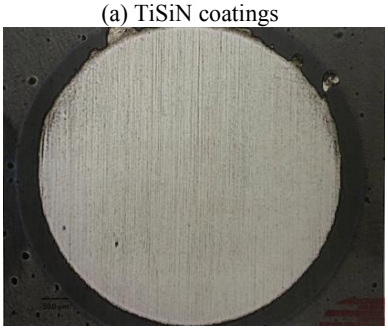

(b) DLC coatings

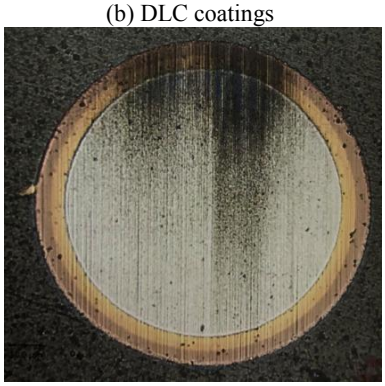

(c) TiSiN/DLC coatings

Figure 9. Calotest images of the resultant coatings (The authors)

F. Nanoindentation Test

The mechanical properties of thin films and coatings, including hardness and modulus, were examined using a conventional indentation technique. This method allows the determination of the intrinsic mechanical properties of the coatings.

Figure 10 presents nanoindentation images of the TiSiN, DLC, and TiSiN/DLC coatings. These images were obtained under a load of 25 mN, allowing for a detailed examination of the indentation behavior of the coatings.

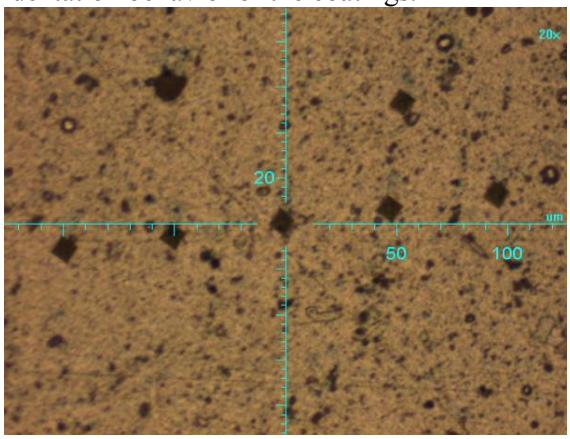

(a)

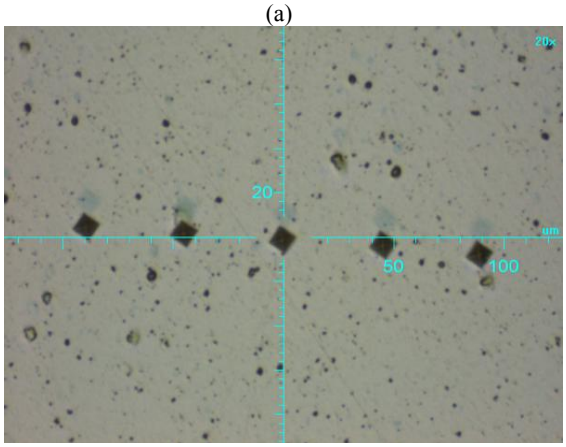

(b)

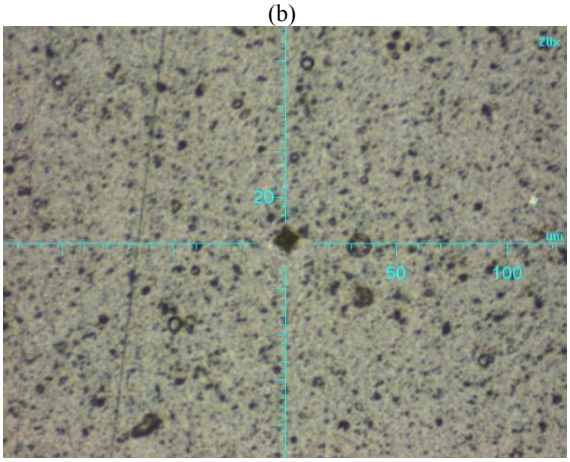

(c)

Figure 10. Nanoindentation images of (a) TiSiN, (b) DLC, and (c) TiSiN/DLC coatings (The authors)

Figure 11 displays the loading and unloading curves of the TiSiN, DLC, and TiSiN/DLC coatings. These curves illustrate the relationship between the applied load and the indentation depth of the coatings. The indentation tests were conducted at various indentation depths, considering the thin coating thickness (as shown

in Table 1), to minimize the substrate effect.

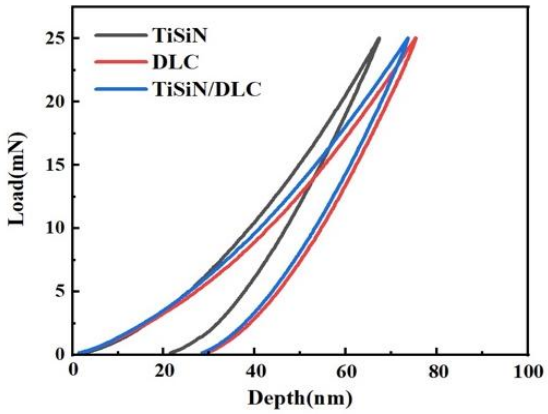

Figure 11. Loading and unloading curves for the resultant coatings (The authors)

Figure 12 shows the mechanical properties of the coatings, including hardness and elastic modulus. The corresponding data are summarized in Table 3.

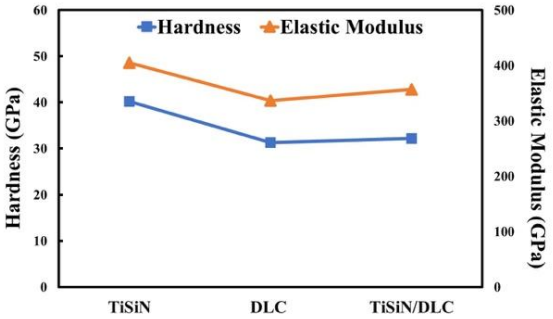

Figure 12. Hardness and elastic modulus of the resultant coatings (The authors)

Table 3.
Mechanical properties of the resultant coatings (The authors)

Coatings	Hardness (H_{IT}) GPa	Elastic Modulus (E_{IT}) GPa	H/E
TiSiN	40.2	405.2	0.0992
DLC	31.3	336.7	0.0930
TiSiN/DLC	32.2	356.8	0.0902

Notably, the TiSiN coatings exhibited remarkable mechanical properties, achieving a maximum superhardness with a hardness value of 40.2 GPa, an elastic modulus of 405.2 GPa, and an H/E ratio of 0.0992. The TiSiN/DLC hybrid coatings demonstrated an improvement in both hardness and elastic modulus compared with the DLC coatings, with a hardness of 32.2 GPa and an elastic modulus of 356.8 GPa. The TiSiN and TiSiN/DLC coatings with (111) and (200) orientations demonstrate higher hardness and modulus values than those reported by [6], [7], [8].

These findings underscore the superior mechanical performance of the TiSiN coating, with the TiSiN/DLC hybrid coatings also offering significant enhancements compared with the DLC coatings. These results are of great significance for applications where hardness and mechanical properties are critical, such as cutting tools in various industries.

IV. Conclusion

In this study, the cathodic arc technique was used to successfully fabricate TiSiN superhard, DLC, and innovative TiSiN/DLC hybrid coatings on tungsten carbide insert cutting tools. The resultant coatings were extensively characterized and evaluated for their structural and intrinsic mechanical properties through nanoindentation testing. The key findings from our experiments can be summarized as follows:

1) Surface morphological analysis using SEM and AFM revealed that the TiSiN coatings effectively inhibited macroparticles, whereas the DLC and TiSiN/DLC hybrid coatings exhibited smoother surfaces with greater density and reduced porosity. Notably, the TiSiN/DLC hybrid coatings exhibited improved surface roughness compared with the TiSiN coatings.

2) The XRD patterns revealed that both TiSiN and TiSiN/DLC hybrid coatings exhibited a preferred orientation along the (111) and (200) crystallographic planes. This orientation was associated with their exceptional hardness and elastic modulus in combination with the substrate. Specifically, the (111) and (200) orientations in the TiSiN and TiSiN/DLC hybrid coatings played a crucial role in achieving their impressive hardness and mechanical properties.

3) Raman spectroscopy results confirmed the DLC nature of the coatings, with characteristic G and D bands confirming their graphitic and disordered carbon structures.

4) Calotest analysis indicated that the DLC coatings were very thin, approximately 1 μm, while the TiSiN/DLC hybrid coatings had a thickness of around 1.8 μm, contributing to their exceptional mechanical properties.

5) Nanoindentation tests showed that the TiSiN coatings achieved a remarkable hardness (HIT) of 40.2 GPa and an elastic modulus of 405.2 GPa through optimized coating conditions. The novel TiSiN/DLC hybrid coatings exhibited enhanced mechanical properties, particularly in terms of hardness and elastic modulus, surpassing those of DLC coatings, making them appealing for various industrial applications.

For accurate nanoindentation testing, it is crucial to ensure that the indentation depth does not exceed 10% of the coating thickness. Going beyond this limit may introduce substrate effects and result in a rapid decrease in hardness values.

In conclusion, this study underscores the promising potential of TiSiN/DLC hybrid coatings for various industrial applications where the performance characteristics of superhard coatings are essential, as seen in TiSiN coatings. Future research should focus on further enhancing the exceptional mechanical and tribological properties and corrosion resistance of these coatings, making them valuable candidates for improving the performance and durability of critical components in cutting tools, automotive applications, medical implants, and other applicable fields.

ACKNOWLEDGMENT

The authors would like to thank Diacoat Technologies Co., Ltd. in Thailand for its invaluable support and expertise in the field of coating and cathodic arc technique. Its contributions and collaboration were instrumental in the successful execution of this study. Its commitment to excellence and technical assistance significantly enhanced the quality of our work. The authors deeply appreciate its dedication and partnership, which made this work possible.

REFERENCES

[1] BROITMAN, E. (2017) Indentation Hardness Measurements at Macro-, Micro-, and Nanoscale: A Critical Overview. *Tribology Letters*, 65 (1), 23.

[2] SHEN, Y.L. (2019) Nanoindentation for Testing Material Properties. In: SCHMAUDER, S., CHEN, C.S., CHAWLA, K., CHAWLA, N., CHEN, W., and KAGAWA, Y. (eds.) *Handbook of Mechanics of Materials.* Singapore: Springer, pp. 1981-2012.

[3] DADA, M., POPOOLA, P., MATHE, N., ADEOSUN, S., and PITYANA, S. (2021) Investigating the elastic modulus and hardness properties of a high entropy alloy coating using nanoindentation. *International Journal of Lightweight Materials and Manufacture*, 4 (3), pp. 339–345.

[4] WEI, Y., LIANG, S., and GAO, X. (2017) Indentation creep of cementitious materials: Experimental investigation from nano to micro length scales. *Construction and Building Materials*, 143, pp. 222–233.

[5] KOPERNIK, M. and MILENIN, A. (2014) Numerical modeling of substrate effect on determination of elastic and plastic properties of TiN nanocoating in nanoindentation test. *Archives of Civil and Mechanical Engineering*, 14 (2), pp. 269–277.

[6] AKHTER, R., ZHOU, Z., XIE, Z., and MUNROE, P. (2021) TiN versus TiSiN coatings in indentation, scratch and wear setting. *Applied Surface Science*, 563, 150356.

[7] DUAN, L., WU, H., GUO, L., XIU, W., and YU, X. (2020) The effect of phase on microstructure and mechanical performance in TiAlN and TiSiN films. *Materials Research Express*, 7, 066401.

[8] MOVASSAGH-ALANAGH, F. and MAHDAVI, M. (2020) Improving wear and corrosion resistance of AISI 304 stainless steel by a multilayered nanocomposite Ti/TiN/TiSiN coating. *Surfaces and Interfaces*, 18, 100428.

[9] YE, Y., YAO, Y., CHEN, H., GUO, S., LI, J., and WANG, L. (2019) Structure, mechanical and tribological properties in seawater of multilayer TiSiN/Ni coatings prepared by cathodic arc method. *Applied Surface Science*, 493, pp. 1177-1186.

[10] HATADA, R., FLEGE, S., ASHRAF, M.N., TIMMERMANN, A., SCHMID, C., and ENSINGER, W. (2020) The Influence of Preparation Conditions on the Structural Properties and Hardness of Diamond-Like Carbon Films, Prepared by Plasma Source Ion Implantation. *Coatings*, 10 (4), 360.

[11] MASASHI, N., SHINGO, K., MINORU, H., and HIDETAKA, A. (2022) Fabrication of nanostructures DLC coatings using anodic alumina films. *Diamond & Related Material*, 126, 109104.

[12] GRIGORIEV, S., VOLOSOVA, M., FYODOROV, S., LYAKHOVETSKIY, M., and SELEZNEV, A. (2019) DLC-coating Application to Improve the Durability of Ceramic Tools. *Journal of Materials Engineering and Performance*, 28, pp. 4415-4426.

参考文:

[1] BROITMAN, E. (2017) 宏观、微观和纳米尺度的压痕硬度测量：关键概述。摩擦学快报，65 (1), 23。

[2] 沉玉兰 (2019) 用于测试材料性能的纳米压痕。见：SCH MAUDER, S.、CHEN, C.S.、CHAWLA, K.、CHAWLA, N.、CHEN, W. 和 KAGAWA, Y.（编辑）《材料力学手册》。新加坡：施普林格，第 1981-2012 年。

[3] DADA, M.、POPOOLA, P.、MATHE, N.、ADEOSUN, S. 和 PITYANA, S. (2021) 使用纳米压痕研究高熵合金涂层的弹性模量和硬度特性。国际轻质材料与制造杂志，4 (3)，第 339–345 页。

[4] 魏Y.，梁S.，高X. (2017) 胶凝材料的压痕蠕变：从纳米到微米尺度的实验研究。建筑和建筑材料，143，第 222-233 页。

[5] KOPERNIK, M. 和 MILENIN, A. (2014) 纳米压痕试验中基体效应对锡纳米涂层弹性和塑性性能测定的数值模拟。土木与机械工程档案，14 (2)，第 269–277 页。

[6] AKHTER, R.、ZHOU, Z.、XIE, Z. 和 MUNROE, P. (2021) 锡与氮化钛涂层在压痕、划痕和磨损情况下的比较。应用表面科学，563, 150356。

[7] DUAN, L., WU, H., GUO, L., XIU, W., 和 YU, X. (2020) 相对氮化钛和氮化钛薄膜微观结构和机械性能的影响。材料研究快报，7，066401.

[8] MOVASSAGH-ALANAGH, F. 和 MAHDAVI, M. (2020) 通过多层纳米复合钛/氮化钛/氮化钛涂层提高美国钢铁协会304不锈钢的耐磨性和耐腐蚀性。表面和界面，18, 100428。

[9] YE, Y., YAO, Y., CHEN, H., GUO, S., LI, J., 和 WANG, L. (2019) 多层氮化钛/你涂层在海水中的结构、机械和摩擦学性能采用阴极电弧法制备。应用表面科学，493，第 1177-1186 页。

[10] HATADA, R.、FLEGE, S.、ASHRAF, M.N.、TIMMERMANN, A.、SCHMID, C. 和 ENSINGER, W. (2020) 制备条件对类金刚石结构性能和硬度的影响碳膜，通过等离子体源离子注入制备。涂料，10 (4)，360。

[11] MASASHI, N.、SHINGO, K.、MINORU, H. 和 HIDETAKA, A. (2022) 使用阳极氧化铝薄膜制造纳米结构DLC涂层。金刚石及相关材料，126, 109104。

[12] GRIGORIEV, S.、VOLOSOVA, M.、FYODOROV, S.、LYAKHOVETSKIY, M. 和 SELEZNEV, A. (2019) DLC涂层应用以提高陶瓷工具的耐用性。材料工程与性能杂志，28，第 4415-4426 页。